pagepress

Geospatial Health 2022; volume 17:1130

The effectiveness of the restricted policy on specific venues in Hong Kong: A spatial point pattern view

Yijia Liu, Wenzhong Shi, Anshu Zhang, Xiaosheng Zhu

Otto Poon Charitable Foundation Smart Cities Research Institute, The Hong Kong Polytechnic University, Hung Hom; Department of Land Surveying and Geo-Informatics, The Hong Kong Polytechnic University, Hung Hom, Hong Kong

Abstract

After the fifth wave of the COVID-19 outbreak in May 2022, the Hong Kong government decided to ease the restrictions policy step by step. The main change was to re-open some venues that people like to visit and extend the hours of operation. With the implementation of the relaxed policy, however, the number of confirmed cases rose again. As a result, further relaxation was delayed. As an evaluation of the effectiveness of the restrictions policy could be a reference for future policies balancing viral spread and functionality of society, this paper aimed to respond to this question from the spatial point distribution view. The time, from late March 2020 to February 2021, during which the related policies took place was divided into six periods based on the policy trend (tightening or relaxing). The two-variable Ripley's K-function was applied for each period to explore the spatial dependence between confirmed cases and venues as changes in the spatial pattern can reveal the effect of the policy. The results show that, as time passed, the clustering degree decreased and reached its lowest level from August to mid-November 2020, then significantly increased, with the extent of clustering becoming more remarkable and the significant cluster size widening. Our results indicate that the policy had a positive effect on suppressing the spread of the virus in mid-July 2020. Then, with the virus infiltrating the community, the policy had little impact on containing the virus but likely contributed to avoid further infection.

Correspondence: Wenzhong Shi, The Hong Kong Polytechnic University, Hung Hom, Hong Kong.
E-mail: lswzshi@polyu.edu.hk

Key words: SARS-CoV-2; spatial point pattern; two-variable Ripley's K function; policy effectiveness; Hong Kong.

Acknowledgements: We sincerely thank the editor, anonymous reviewers, and Ph.D. candidate, Miss. Tan Xiaoyue for their comments and suggestions that significantly improved the manuscript.

Funding: This study was supported by the Research Grants Council, HKSAR Government (C5079-21G), the Innovation and Technology Commission, HKSAR Government (ITP/041/21LP), and Otto Poon Charitable Foundation Smart Cities Research Institute, the Hong Kong Polytechnic University (CD03).

Conflict of interest: The Authors declare no conflict of interest.

Received for publication: 5 July 2022.
Revision received: 2 November 2022.
Accepted for publication: 9 November 2022.

Geospatial Health 2022; 17:1130
doi:10.4081/gh.2022.1130

Introduction

Affected by the coronavirus 2019 (COVID-19), caused by the severe acute respiratory syndrome coronavirus 2 (SARS-CoV-2), human society has not yet fully returned to normal. Since the first case was confirmed on 23 January 2020 in Hong Kong, this area has suffered from five waves of severe outbreaks. World Health Organization (WHO) has determined that the mode of transmission includes human close physical contact, long-range airborne and fomite contact (WHO, 2020). All these are more likely to happen in poorly ventilated or crowded indoor settings. As a result, such venues, e.g., restaurants, put people at risk. From March 2020, with the intention of reducing infections as well as taking the impact on the economy into account, the Hong Kong government (HKG) implemented a number of restrictions (hereafter called 'the policy') on the operation mode of such venues, such as limited accommodation per table, shortened opening hours or only allowing take away food and so on (HKG, 2020a).

By April 2022, the number of daily cases of the fifth wave was down to an average of one hundred, so the HKG began easing most of the restrictions phase by phase. The first phase allowed part of premises to re-open and the daily confirmed cases were stable in the following days. However, when the second phase started on 19 May 2022, the daily confirmed cases gradually climbed to around two thousand. Among them, around one hundred cases were related to clubs (HKG, 2022), which again highlighted the infection risk of being exposed to crowded venues. Consequently, the HKG announced maintaining the existing anti-epidemic rules; further relaxation would be delayed. The question then was: if the situation gets worse, should we tighten the policy again? Since the

restriction policy had been executed from 2020, it is worthwhile to identify the effectiveness of the policy from the past to guide the future. From a spatial analysis view, with tightening or relaxing of the policy, the corresponding spatial point pattern between venues and cases would be changed. We focused on this issue since an understanding of the changes can provide insights into the effectiveness of the policy.

Materials and Methods

Study area

Hong Kong, the Special Administrative Region of China, was the study area for this study. More than 7.4 million people live in this highly urbanized city, which has an area of 1104 km^2. Since we wished to apply the Ripley's K-function (see below), which is based on Euclidean distance, areas of the sea can affect the analysis results. Therefore, the whole of Hong Kong was divided into three parts (A, B and C, where the land boundary sizes relate as 10, 1, 2, respectively) as shown in Figure 1. Here, we mainly discuss the results in the largest land area A, which represented most of the confirmed cases (Table 1). Therefore, the results in area A can be seen as a reasonable proxy of the whole of Hong Kong. No experiment was carried out in area C (Lantau Island), because most of this area is mountainous with too few cases and points of interest (POIs) with respect to potential virus transmission to form spatial patterns. A similar problem also occurred in area B as no regular spatial pattern could be expected there due to the lack of POIs. The exact number of POIs is listed in Table 1.

Data source and preprocessing

All confirmed case information was obtained from the Hong Kong COVID-19 thematic website (HKG, 2020b). Data recorded detailed information, case number (*i.e.* the unique number assigned to each case), residential address (*i.e.* where the person in question lived when the diagnosis was confirmed), the date when the case was confirmed and the type of case (*i.e.* local case, epidemiologically linked with local case, imported case or epidemiologically linked with imported case) were used in this study. The corresponding latitudes and longitudes of address were obtained from Google Maps Geocoding API. A total of ten types of POIs data involved by the policy were collected from the Hong Kong GeoData Store (HKG, 2019) and Google Maps.

The population density data, as shown in Figure 2, was obtained from government open data source at Tertiary Planning Unit (TPU) level for the purpose of representing spatial heterogeneity purpose (HKG, 2016), which would be explained further in the *Method* section, while the physical boundaries were extracted from the Hong Kong official digital boundaries (HKU, GIS Research Centre, 2016).

By making use of the HKG News Website (HKG, 2002), the relevant policies from March 2020 to February 2021 were collected. Based on the policy trends, six durations were divided as shown in Figure 3.

Methodological approach

Ripley's K-function is a powerful tool for exploring the second-order behavior of spatial point patterns (Ripley, 1977). Not limited by administrative boundaries, this method can measure on a continuous scale. Researchers developed different versions of this method to deal with various situations, e.g., a comprehensive review was conducted by Marcon and Puech (2017). Applications of this approach in geographical epidemiology can be traced back to the early 1960s, e.g., a study was designed to examine whether clustering existed in child cancer distribution in the Penwortham (Gatrell *et al.,* 1996), while a much later study shows that the establishment of the Xiaotangshan Hospital during the SARS epidemic reduced clustering significantly (Cao *et al.,* 2017). Here, we adopted one of the extensions, called cross-K-function or two-variable Ripley's K-function, which can be estimated by:

$$\hat{K}_{12}(r) = (n_1 n_2)^{-1} |A| \sum_{i=1}^{n_2} \sum_{j=1}^{n_1} W_{ij}^{-1} I(d_{ij} \leq r) \quad (1)$$

where r is the research radius; n_1 and n_2 the number of research objects 1 and 2, respectively; A the research area; d_{ij} the Euclidean distance between point i and point j; I an indicator function, when $d_{ij \leq r}$ equals 1 and 0 otherwise; and W_{ij} a edge correction factor.

In this study, we consider confirmed cases as n_1, and each type of POIs as n_2. The basic idea of the K-function is to identify the spatial dependence between n_1 and n_2, if there is one. A report from WHO (2020) claims that the incubation period for SARS-CoV-2 is 5 – 6 days on average, while the interval from symptom onset to diagnosis to final reporting in Hong Kong has been found to be around 4 days (Leung *et al.,* 2021). To take this delay into account, we set 10 days as the total lag period, that is, for each confirmed case, the 10 days following it were considered to represent the current situation. Besides, to reveal the reality better, the imported cases and the cases in Quarantine Centers who did not interact with society were excluded. The processed data for each duration of infection and area are shown in Figure 3. Following the results by *Moovit,* an international mobility services provider (self-claimed to be 'The Most Popular Urban Mobility Application in Hong Kong') that applies statistics and analytics for calculation of average public trip distance based on application usage data (Moovit, 2021), this paper set the detection range at 8 km. As recommended by the official R document (DataCamp, 2020), Ripley's isotropic correction was used for edge correction. A common linear transformation called the L-function can be used to obtain a constant variance and better visualization. The definition can be expressed as:

Table 1. The number of each type of identified POI in area A and area B.

No.	Types of POI	Numbers	
		A	B
1.	bathhouse	91	20
2.	beauty parlor	88	26
3.	club or nightclub	63	21
4.	fitness center	124	39
5.	amusement games center	112	30
6.	karaoke establishment	46	27
7.	mahjong-tin kau premises	68	13
8.	massage establishment	86	19
9.	"party room"	94	13
10.	public entertainment	72	28

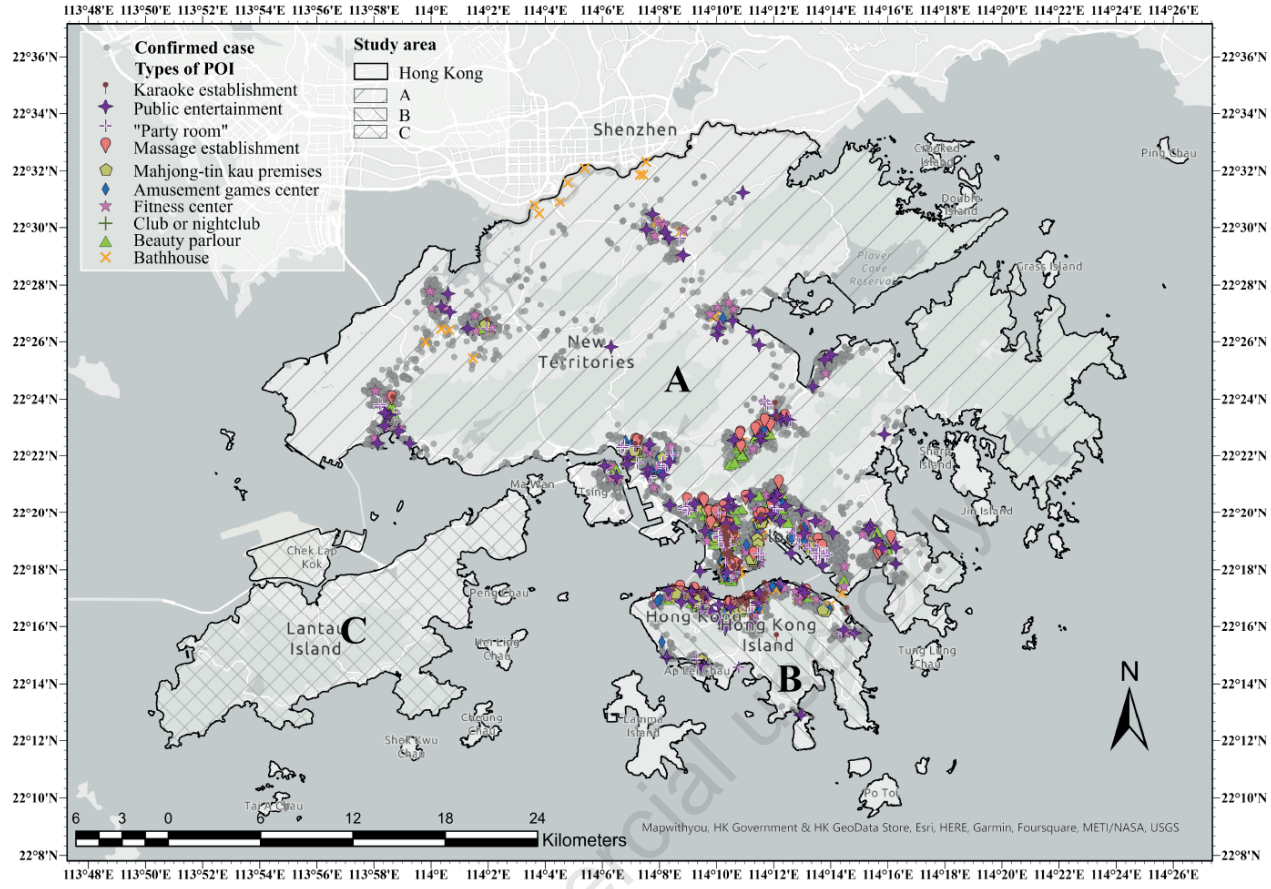

Figure 1. Distribution of confirmed cases and ten types of POI in the study area.

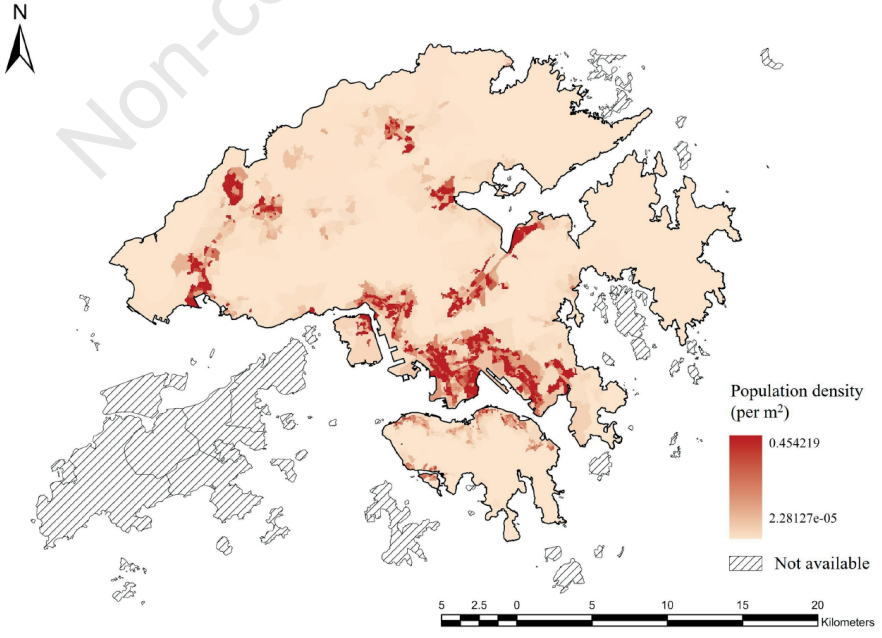

Figure 2. Population density distribution in the study area.

$$\hat{L}_{12}(r) = \sqrt{\hat{K}_{12}(r)/\pi} - r \quad (2)$$

To test the significance of the results, 99 Monte Carlo randomizations were simulated to build 99% confidence envelopes. By default, the simulative point pattern would follow complete spatial randomness (CSR) pattern (Oro *et al.,* 2012; Zhang *et al.,* 2020). This assumes that the point pattern expresses stationarity and is isotropic. However, the assumption of stationarity may not be acceptable in reality application due to the underlying spatial heterogeneity of the intensity. As in this study, both population and POI distribution are far away from the CSR pattern and any deviation from CSR would affect the result. To exclude this effect, the key idea is to find an appropriate substitute. One approach would be to conduct other investigations to establish reasonable simulations (Arbia *et al.,* 2012; Liu *et al.,* 2007) using existing data to build up simulations (Lentz *et al.,* 2011; Ruiz-Moreno *et al.,* 2010). The latter approach was adopted in this study. The infection is highly related to population density, so we assumed the actual distribution of population density could reflect the underlying point process of cases. Additionally, the case-control design was applied. In each simulation, the POI locations were fixed and the same number of cases were generated from population density distribution. In one separate set of 99 simulations, the maximum and minimum values obtained were set as the upper and lower envelope curves, while in the other separate set of 99 simulations, the average of these simulated values was taken as the theoretical mean value. If an observed $\hat{L}_{12}$ value is above the upper envelope curve, the pattern is regarded as a clustered distribution, while as a discrete one if below the lower envelope curve; otherwise it would be regarded as a random distribution.

Software

All data processing work was realized using Python 3.5 (https://www.python.org/downloads/release/python-350/), while spatial analysis utilized the R studio '*spatstat*' package (Baddeley & Turner, 2005; Baddeley *et al.,* 2016).

Results

Figure 4 summarizes the results, which emphasizes the calculation results for each specific type of POI. In the first duration (Figure 4A), all the observed values within the confidence envelopes showed a random situation indicating that the distribution between confirmed cases and POIs was not related. From the second duration, with exception of the distributions involving beauty parlors, "party rooms" and areas for public entertainment in the fourth duration, the observed values were higher than the upper envelope boundary in a specific range, showing a spatial clustering pattern. The overall clustering degree, defined as the maximal deviation between the observed value and the upper envelope boundary, decreased at first (Figure 4B to D) then markedly increased (Figure 4D to F). The extent of clustering, defined as the maximal range of observed value beyond the confidence bounds, was at 4 to 8 km at the beginning (Figure 4B and C), then gradually expanded to the whole range (Figure 4E and F).

In mid to late March, a cluster of local cases involving bars and clubs broke out. The government then successively announced the temporary closure of specific venues. Associated with the result of the first duration, the random distribution may support the effect of policy, as the other study claimed (Lam *et al.,* 2020), but it is more likely that there were too few cases around to form a reliable dis-

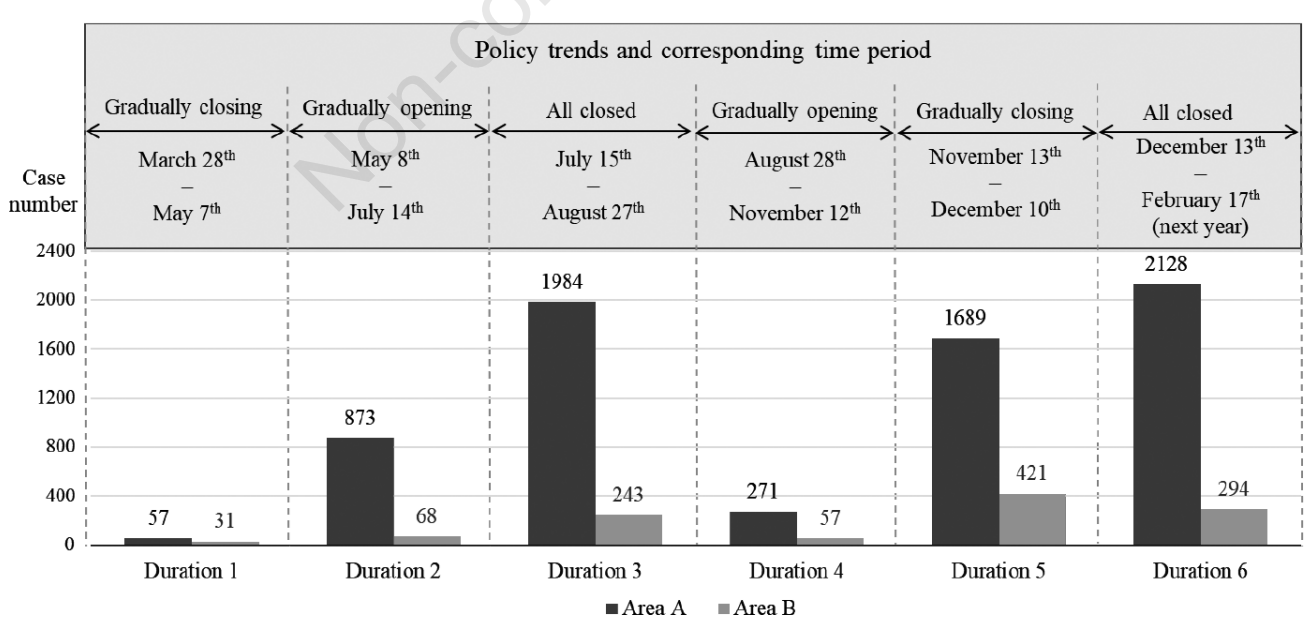

Figure 3. The number of confirmed cases in six durations in study area A and area B. The corresponding policy trends and time periods are listed above.

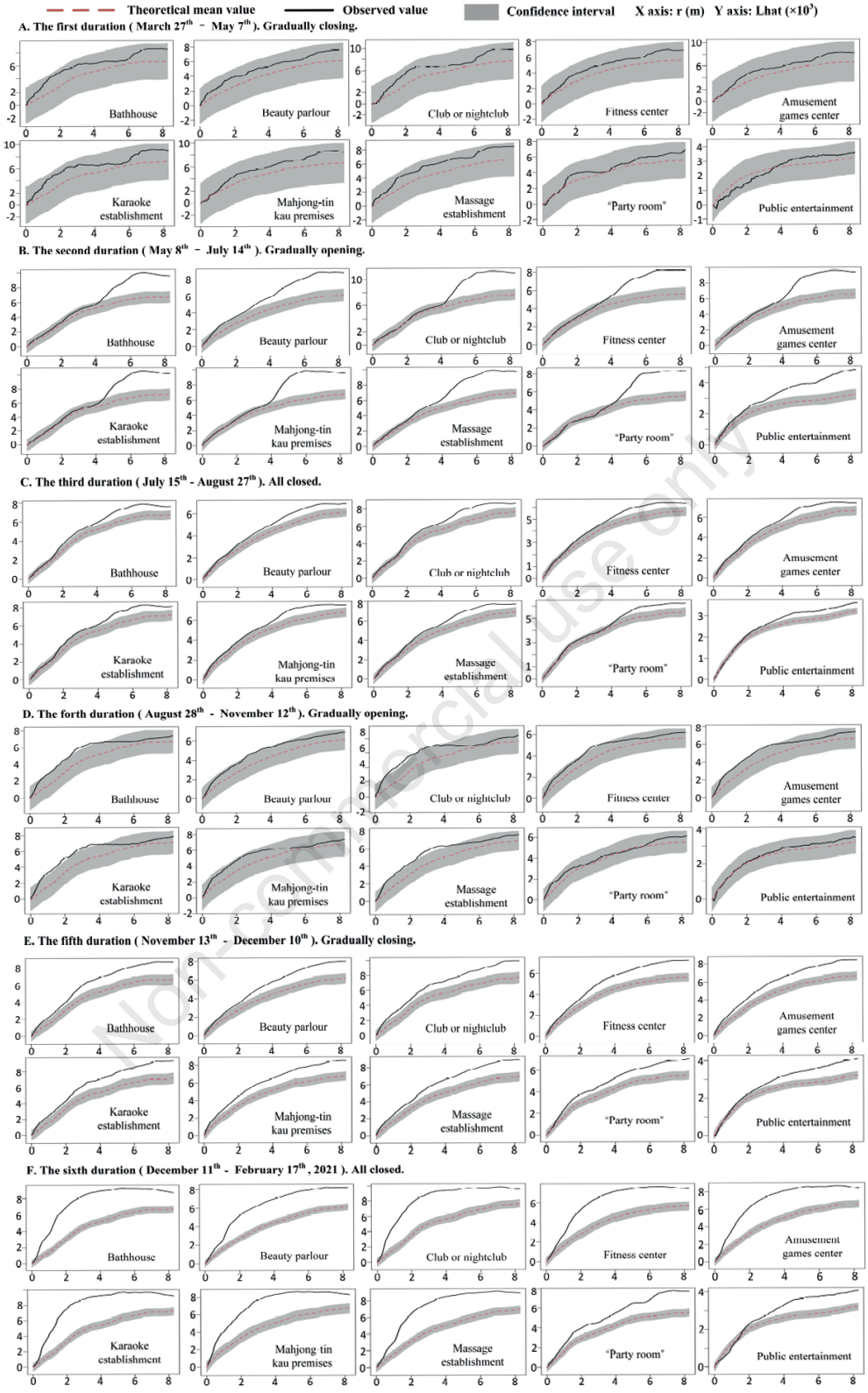

Figure 4. Ripley's K function calculation result for each duration. Sub-title indicated the duration and the corresponding policy trend. In each sub-figure, the solid black line was the observed value, while the red dash line was the theoretical value. The grey part meant the confidence envelopes. The horizontal axis represented the detection range r (m), while the vertical axis represented the calculated result $\hat{L}$ (×10³).

tribution. With the gradually relaxing trend in the second duration, a significant clustering was detected at 4 to 8 km. This result indicates that transmission had already been generated at long-range scales considering POIs heralding future outbreaks. The inference was supported by the higher daily confirmed cases in the next duration. The total number doubled in the third duration as well. Next, although the number of daily confirmed cases in the third duration climbed to a historically highest level, the clustering degree was mitigated compared to the previous duration. This result reflects the effectiveness of the closure of venues.

Importantly, around mid-November, a few cases visited 28 bars, karaoke clubs, and fitness centers, resulting in a vast group infection affecting 732 people, called the 'Dancing/Singing cluster' in the government official report (HKG, 2020b). By further comparing the unique case number, 11% of people in the infected group were involved in the analysis of this duration. Therefore, in the fourth duration, our result observed corresponding clustering distribution in related venues (Figure 4 D. club or night club, fitness center, and karaoke establishment). However, our result also identified a clustering involving bathhouses, massage establishments, and amusement game centers. When the time came to the fifth and sixth duration, the overall epidemic situation deteriorated. On the one hand, the clustering degree in the long-range was stronger. In the infected group people, 63% were included in the analysis of this duration. Thus, the reason for the higher clustering is highly likely to have been caused by more and more people confirmed to be involved in the 'Dancing/Singing cluster' got. On the other hand, clustering also showed up at relatively small scales. This may be a sign that the virus transmission characteristic changed from far to close locations in relation to the POIs.

Discussion

In Hong Kong, the anti-pandemic progress is entering its third year. The relaxation process was delayed because of the emergence of group infections. To guide policy decisions in the future, the experience from the last two years is useful. Our result detected significant clustering in the second duration, echoing a previous finding that the entertainment environment dominated the transmission from January to June in Hong Kong (Wong *et al.,* 2020). In the third duration, the decrease of the degree of clustering emphasized the effectiveness of the lockdown policy, although the total number of confirmed cases was higher. One explanation could be that the prevalent transmission shifted from entertainment settings to residence clusters in the period of June to October (Kwan *et al.,* 2022). Results from the fourth duration also indicate that there existed other high-exposure risk venues. A detailed study of people's daily travel trajectory may help identify whether they paid exceptional visits to such venues.

As the 'Dancing/Singing' cluster mainly coincided with the increased transmission in the fifth and sixth durations, a link involving the location of POIs with the residents' socioeconomic status (SES) could perhaps explain the expansion of the clustering extent. This line of research was followed by Zhang *et al.* (2022), who claimed that the virus had spread from high-income to lower-income populations in late November 2020. They also pointed out that high-income people live in less densely populated areas, far from entertainment venues but with high accessibility. Infected people from these areas might have initially spread the virus to the venues they visited more frequently leading to secondary transmission hubs involving people living near commercial and entertainment areas. Further transmission would then reach residents with lower-SES living close to these venues and are more vulnerable to COVID-19, thereby setting off cross-neighbourhood infections with more robust clustering in the sixth duration.

Despite the gradual lockdowns beginning in late November, this did not stop the spread of the virus since community transmission now dominated. Note that this does not mean the policy is ineffective, but the role played by the policy changed from reducing transmission, as in late July, to avoiding more potential infections. Therefore, other prevention policies aimed at the community level should be contemplated. Since the result strongly depends on the primary distribution, the comparison between various venues in the same duration may be unreliable. Moreover, as of 27 February 2021, only 3% of the total number of people had received the first shot of the vaccine (Our World in Data, 2019), and the impact was too minimal to be counted during the study period.

This study has limitations. First, the record locations of the confirmed case were their residences rather than the actual place where they got infected, which limited the accuracy of the result to some extent. Also, the difference in transmissibility of SARS-CoV-2 variants were not considered. Since the result is highly dependent on the initial spatial point pattern, its generalizability may be limited.

Conclusions

This study examined the effectiveness of restrictions policy from a spatial point distribution view. Our result verified the positive effect of suppressing the virus spread from mid-July to August 2020, which was more likely to play a preventive role against further infections from late 2020 to early 2021. However, when the virus made inroads at the community level, other policies aimed at that level should have been considered. The effect of the overall policy implemented was assessed to provide a reference for government attempts to optimize COVID-19 control policy in the future.

References

Arbia G, Espa G, Giuliani D, Mazzitelli A, 2012. Clusters of firms in an inhomogeneous space: The high-tech industries in Milan. Econ Model 29:3-11.

Baddeley A, Rubak E, Turner R. 2016. In Spatial Point Patterns. Methodology and Applications with R, 828 pp. Chapman and Hall/CRC, Boca Raton, USA, 2015.

Baddeley A, Turner R, 2005. spatstat: An R Package for Analyzing Spatial Point Patterns. J Stat Softw 12:1-42.

Cao Z, Zhao P, Liu J, Zhong W, 2017. A Spatial Point Pattern Analysis of the 2003 SARS Epidemic in Beijing EM-GIS'17: Proceedings of the 3rd ACM SIGSPATIAL Workshop on Emergency Management using, Redondo Beach, CA, USA. Article No.: 1:1–8. Doi: 10.1145/3152465.3152466

DataCamp, 2020. Rdocumentation. Accessed: 2021 June 23. Available from: https://www.rdocumentation.org/packages/spatstat/versions/1.64-1/topics/Kcross.

Gatrell A C, Bailey TC, Diggle PJ, Rowlingson BS, 1996. Spatial point pattern analysis and its application in geographical epidemiology. Trans Inst Br Geogr 21:256-74.

HKG, 2002. NEWS. Accessed: 2021 May 7. Available from: https://www.news.gov.hk/eng/index.html.

HKG, 2016. Census and Statistics Department. District Profiles. Population By-census. Available from: https://www.bycensus2016.gov.hk/en/bc-dp-tpu.html. Accessed: 2021 May 6.

HKG, 2020a. Prevention and Control of Disease (Prohibition on Gathering) Regulation. Accessed: 2021 April 15. Available from: https://www.elegislation.gov.hk/hk/cap599G

HKG, 2020b. Together, We Fight the Virus!. Accessed: 2021 April 10. Available from: https://www.coronavirus.gov.hk/eng/.

HKG, 2022. 446 COVID-19 cases recorded. Accessed: 2022 June 4. Available from: https://www.news.gov.hk/eng/2022/06/20220604/20220604_165906_820.html

HKG, Lands Department, 2019. Hong Kong geodata store. Accessed: 2020 March 20. Available from: https://geodata.gov.hk/.

HKU, GIS Research Centre. 2016. Major Data Sources in Hong Kong: Planning Department - Digital boundary of Town Planning Unit (TPU) and Street Block (SB). Accessed: 2021 March 20. Available from: http://www.dupad.hku.hk/cusup/hkugis/html/Data.html

Kwan TH, Wong NS, Yeoh EK, Lee SS, 2022. Shifts of SARS-CoV-2 exposure settings in the transmission clusters of 2 epidemic waves in Hong Kong. Int J Environ Health Res 18:1-13.

Lam HY, Lam TS, Wong CH, Lam WH, Leung CME, Au KWA, Lam CKY, Lau TWW, Chan YWD, Wong KH, Chuang SK, 2020. The epidemiology of COVID-19 cases and the successful containment strategy in Hong Kong-January to May 2020. Int J Infect Dis 98:51-8.

Lentz JA, Blackburn JK, Curtis AJ, 2011. Evaluating patterns of a white-band disease (WBD) outbreak in Acropora palmata using spatial analysis: a comparison of transect and colony clustering. PLoS One 6:e21830.

Leung K, Wu JT, Leung GM, 2021. Real-time tracking and prediction of COVID-19 infection using digital proxies of population mobility and mixing. Nat Commun 12:1501.

Liu D, Kelly M, Gong P, Guo Q, 2007. Characterizing spatial–temporal tree mortality patterns associated with a new forest disease. For Ecol Manag 253:220-31.

Marcon E, Puech F, 2017. A typology of distance-based measures of spatial concentration. Reg Sci Urban Econ 62:56-67.

Moovit, 2021. Public transit statistics by country and city. Accessed: 2021 June 15. Available from: https://moovitapp.com/insights/en/Moovit_Insights_Public_Transit_Index-countries.

Oro FZ, Bonnot F, Ngo-Bieng MA, Delaitre E, Dufour BP et al., 2012. Spatiotemporal pattern analysis of cacao swollen shoot virus in experimental plots in Togo. Plant Pathology 61:1043-51.

Our World in Data. 2019. Coronavirus (COVID-19) Vaccinations. Accessed: 2022 June 15. Available from: https://ourworldindata.org/covid-vaccinations?country=HKG.

Ripley BD, 1977. Modeling Spatial Patterns. J R Stat Soc B Stat Methodol 39:172-212.

Ruiz-Moreno D, Pascual M, Emch M, Yunus M, 2010. Spatial clustering in the spatio-temporal dynamics of endemic cholera. BMC Infect Dis 10:51.

WHO, 2020. Coronavirus disease 2019 (COVID-19) Situation Report – 73. Accessed: 2020 May 10. https://www.who.int/docs/default-source/coronaviruse/situation-reports/20200402-sitrep-73-covid-19.pdf

Wong NS, Lee SS, Kwan TH, Yeoh EK, 2020). Settings of virus exposure and their implications in the propagation of transmission networks in a COVID-19 outbreak. Lancet Reg Health West Pac 4:100052.

Zhang AS, Shi WZ, Tong CZ, Zhu XS, Liu YJ, Liu ZW, Yao YP, Shi ZC, 2022. The fine-scale associations between socioeconomic status, density, functionality, and spread of COVID-19 within a high-density city. BMC Infect Dis 22:274.

Zhang X, Yao J, Sila-Nowicka K, Song C, 2020. Geographic concentration of industries in Jiangsu, China: a spatial point pattern analysis using micro-geographic data. Ann Reg Sci 66:439-61.